

DogFit: Domain-guided Fine-tuning for Efficient Transfer Learning of Diffusion Models

Yara Bahram, Mohammadhadi Shateri, Eric Granger

LIVIA, ILLS, ETS Montreal, Canada

yara.mohammadi-bahram@livia.etsmtl.ca, {mohammadhadi.shateri, eric.granger}@etsmtl.ca

Abstract

Transfer learning of diffusion models to new domains with limited data is challenging, as naively fine-tuning the model often results in poor generalization. Test-time guidance methods help mitigate this by offering controllable improvements in image fidelity through a trade-off with sample diversity. However, this benefit comes at a high computational cost, typically requiring dual forward passes during sampling. We propose the Domain-guided Fine-tuning (DogFit) method, an effective guidance mechanism for diffusion transfer learning that maintains controllability without incurring additional computational overhead. DogFit injects a domain-aware guidance offset into the training loss, effectively internalizing the guided behavior during the fine-tuning process. The domain-aware design is motivated by our observation that during fine-tuning, the unconditional source model offers a stronger marginal estimate than the target model. To support efficient controllable fidelity–diversity trade-offs at inference, we encode the guidance strength value as an additional model input through a lightweight conditioning mechanism. We further investigate the optimal placement and timing of the guidance offset during training and propose two simple scheduling strategies, i.e., *late-start* and *cut-off*, which improve generation quality and training stability. Experiments on DiT and SiT backbones across six diverse target domains show that DogFit can outperform state-of-the-art guidance methods in transfer learning in terms of FID and FD_{DINOv2} while requiring up to $\sim \times 2$ fewer sampling TFLOPS.

Code — <https://github.com/yaramohamadi/DogFit>

Introduction

Denoising diffusion probabilistic models (DDPMs) (Sohl-Dickstein et al. 2015; Ho, Jain, and Abbeel 2020) have emerged as powerful generative models, achieving state-of-the-art (SOTA) results in image synthesis (Dhariwal and Nichol 2021; Rombach et al. 2022), video generation (Gupta et al. 2024; Ho et al. 2022), and image editing (Kawar et al. 2023). However, producing high-quality and diverse outputs still requires substantial computational and data resources, particularly with large diffusion backbones and image sizes. In practical applications such as personalized generation with limited data, full model training from scratch is

Copyright © 2026, Association for the Advancement of Artificial Intelligence (www.aaai.org). All rights reserved.

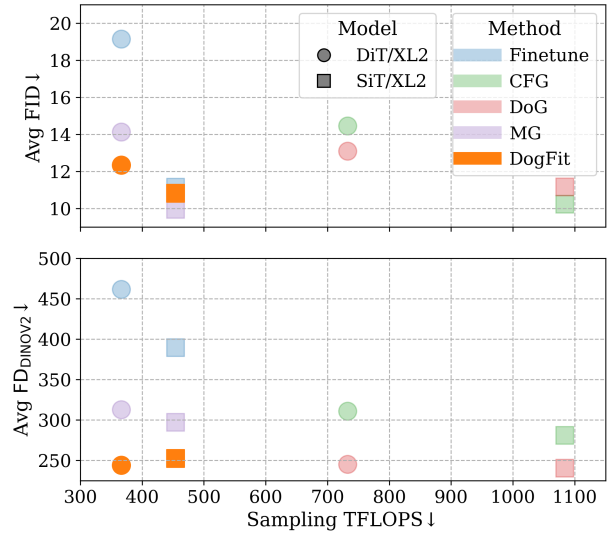


Figure 1: DogFit outperforms SOTA guidance methods in majority of cases for diffusion transfer learning, without increasing sampling overhead (TFLOPS). Evaluation is based on FID and FD_{DINOv2} averaged across six target datasets.

infeasible, making transfer learning a critical tool for target adaptation. A common approach in this setting is to fine-tune a pre-trained diffusion model on the target data. While straightforward, this strategy frequently suffers from overfitting and poor generalization due to the limited size and diversity of the target domain.

Classifier-free guidance (CFG) is a standard technique for improving generation quality at inference time by modulating the conditional signal (Ho and Salimans 2022; Karras et al. 2024). This technique is often used in its original form even after target adaptation to steer the model towards better generalization. However, CFG assumes access to well-trained conditional and unconditional models, which is difficult to ensure in transfer scenarios where the target domain is small or lacks labels (Ho and Salimans 2022; Zhong et al. 2025). Recent methods like domain guidance (DoG) address these issues by utilizing the unconditional source model as a

stronger marginal noise estimator, offering improved target domain alignment and generalization (Zhong et al. 2025; Phunyaphibarn et al. 2025). Nevertheless, both CFG and DoG introduce significant computational overhead at sampling time due to their reliance on dual forward passes (Ho and Salimans 2022; Zhong et al. 2025). On the other hand, model guidance (MG) mitigates CFG’s runtime cost in in-domain settings by injecting the guidance signal directly into the diffusion training objective (Chen et al. 2025; Tang et al. 2025). However, MG inherits the limitations of CFG in transfer learning due to the underfitting of the unconditional noise estimator (Zhong et al. 2025). Further, MG hard-codes the guidance strength value during training, restricting control at inference. These limitations raise a key question: *can we design effective guidance mechanisms for diffusion transfer learning without incurring computational overhead and still maintaining controllability over the guidance strength?*

This paper proposes domain-guided fine-tuning (DogFit), a method that injects a domain-aware guidance offset into the training loss during the fine-tuning process. This allows the diffusion model to directly learn the guided direction, removing the need for additional test-time processes. The domain-aware design is motivated by our observation that during fine-tuning, the source model offers stronger marginal noise estimates than the evolving target model. This design encourages the model to step toward the target domain manifold and avoid out-of-distribution generation. To support efficient control over the guidance strength at inference, DogFit conditions the model on the guidance value and exposes it to a range of such values during training. This allows the model to modulate its generation behavior accordingly, enabling fidelity–diversity trade-offs at inference with negligible sampling overhead. We further investigate the optimal placement and timing of the guidance offset during training. Two cost-effective guidance scheduling mechanisms are proposed for DogFit: (1) a *late-start* strategy that delays guidance until the model has learned sufficiently stable target representations; and (2) a *cut-off* scheme that restricts guidance to the later denoising steps, where fine-grained domain-specific details are more prevalent. Results over six datasets with different distribution shifts and supervision levels, using two SOTA diffusion backbones, DiT (Peebles and Xie 2023) and SiT (Ma et al. 2024), show that DogFit can outperform SOTA guidance methods in terms of FID and FD_{DINOv2} while reducing their sampling TFLOPS by up to $2\times$ (Fig.1). Results establish DogFit as a practical and efficient guidance method for diffusion transfer learning.

Contributions. (i) We propose DogFit, a training-time guidance mechanism for diffusion transfer learning that enables controllable improvement over target domain generation fidelity without requiring additional processes or double forward passes at test-time. (ii) We show that, during fine-tuning, the source domain model offers stronger marginal estimates than the target model, making it better suited for generating guidance signals. We empirically analyze how the timing and placement of this guidance impact training and propose two scheduling strategies that enhance training

stability and generation quality. (iii) Extensive experiments are conducted across diverse target datasets on DiT and SiT diffusion backbones, showing that DogFit can outperform SOTA guidance methods in transfer learning.

Related Work

Efficient Diffusion Models. The iterative denoising process in diffusion models imposes high sampling-time costs (Shen et al. 2025). To accelerate generation, prior work reduces the number of sampling steps via improved solvers (Song, Meng, and Ermon 2020; Lu et al. 2022), optimized noise schedules (Zheng et al. 2023), or distillation-based methods that train few(one)-step student models to mimic large multi-step teachers (Salimans and Ho 2022; Yin et al. 2024). Recent efforts (Jensen and Sadat 2025; Hsiao et al. 2024; Zhou et al. 2025) distill CFG to eliminate test-time dual passes. Our method, similar to CFG distillation, aims to internalize guidance, but does so without the architectural modifications or post-hoc training stages required by distillation methods. Instead, DogFit simply integrates guidance directly into the fine-tuning objective.

Diffusion Transfer Learning. Transfer learning adapts a model pre-trained on a large-scale source domain to a target domain with smaller size and diversity, leveraging learned representations for better generalization (Weiss, Khoshgof-taar, and Wang 2016). In the context of diffusion models, strategies broadly fall into three categories: Parameter-efficient fine-tuning (PEFT) methods reduce training cost by limiting the number of trainable parameters, often via adapters or LoRA (Hu et al. 2022; Xie et al. 2023; Moon et al. 2022). Distillation-based methods preserve pre-trained source priors during adaptation, particularly during early denoising steps (Zhong et al. 2024; Hur et al. 2024). Few-shot image generation methods enable diffusion models to generalize to unseen domains using a handful of images (Zhu et al. 2022; Wang et al. 2024; Cao and Gong 2024; Ouyang et al. 2024; Ruiz et al. 2023). Despite this progress, current methods overlook the role of guidance in shaping the generation trajectory, implicitly assuming that its original form remains optimal after adaptation, a limiting assumption in small, low-diversity target domains. We propose a new guidance method tailored for diffusion transfer that can be layered on top of existing fine-tuning methods for improving generalization without incurring additional sampling cost.

Proposed Method

Let ϵ_{θ_0} denote a diffusion model pre-trained on a large-scale source domain \mathcal{D}^S , and let \mathcal{D}^T be a smaller target domain such that $|\mathcal{D}^T| \ll |\mathcal{D}^S|$ (typically, $1000 < |\mathcal{D}^T|$). The goal of transfer learning is to fine-tune a model ϵ_{θ} (initialized with the weights θ_0 of the pre-trained model) on \mathcal{D}^T such that it generates high-quality, diverse samples aligned with the target distribution $p(x|\mathcal{D}^T)$. In this work, we aim to develop a strong guidance mechanism for diffusion transfer learning that is computationally efficient and supports controllable guidance strength.

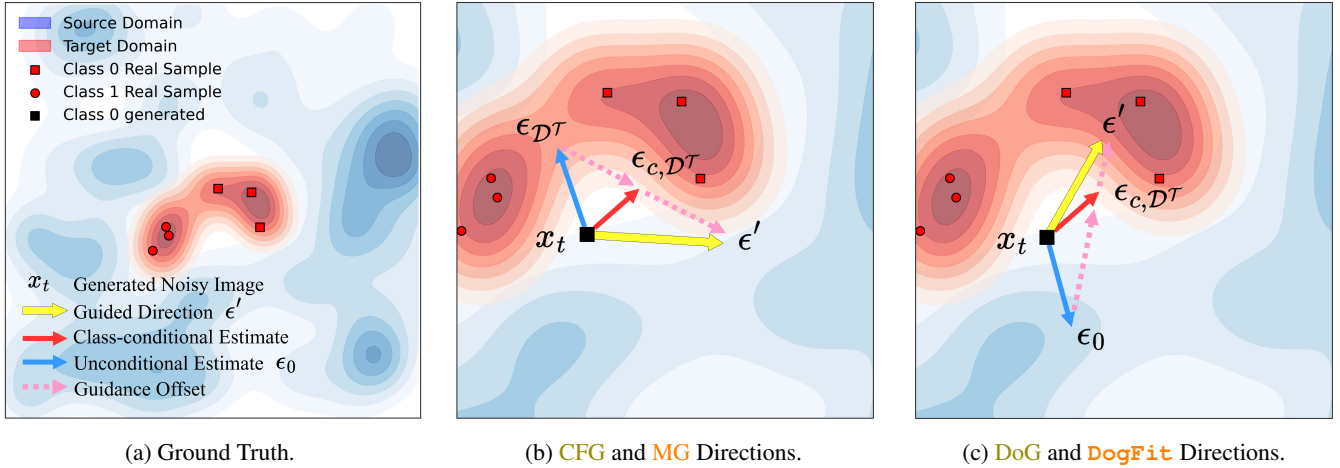


Figure 2: Transfer learning via guidance mechanisms for synthetic data created using a mixture of Gaussian distributions. (a) The red region defines the target domain, while the blue background represents the source distribution. (b) CFG and MG prioritize class separability without considering the source distribution, often pushing samples toward out-of-distribution areas in the target domain. (c) **DoG** and **DogFit** utilize source information to emphasize movement towards the core of the target manifold, improving domain alignment. (*) **Sampling-time** guidance methods (DoG and CFG) operate by computing the **guidance offset**, whereas **training-time** guidance methods (**DogFit** and MG) learn the **guided direction** directly.

Preliminaries

Diffusion Models. Denoising Diffusion Probabilistic Models (DDPMs) (Ho, Jain, and Abbeel 2020) are generative models that learn to reverse a fixed noising process applied over T time-steps. Starting from a clean image x_0 , noise is gradually added to produce a sequence of noisy images $\{x_t\}_{t=1}^T$. A neural network $\epsilon_\theta(x_t, t)$ is trained to predict the noise ϵ at each time-step t , using this denoising objective:

$$\mathcal{L}_{\text{simple}} = \mathbb{E}_{t, x_0, \epsilon} [\|\epsilon_\theta(x_t, t) - \epsilon\|^2]. \quad (1)$$

Time-step t is omitted in subsequent sections when clear from context. In conditional generation, the model receives an auxiliary input c (e.g., class labels or text), producing $\epsilon_\theta(x_t | c)$. SOTA transformer-based diffusion architectures such as DiT (Peebles and Xie 2023) and SiT (Ma et al. 2024) operate in latent space rather than directly on pixel space. For notational simplicity, however, we keep using x to denote the model input.

Guidance in Transfer Learning. While diffusion models can functionally incorporate conditional inputs during training, their outputs often drift under weak conditioning, motivating the use of guidance signals during the reverse process (Dhariwal and Nichol 2021; Ho and Salimans 2022). We present three representative guidance strategies in transfer learning (i.e., CFG, MG, and DoG) covering the main design axes: *where* the guidance signal originates (unconditional branch, or external source model) and *when* it is injected (sampling-time vs. training-time). See visual comparison in Fig. 2.

- **Classifier-Free Guidance (CFG)** (Ho and Salimans 2022; Nichol et al. 2021) improves conditional generation by extrapolating the model’s class-conditional prediction further away from its unconditional counterpart—typically using the

same model. The reverse process is modified as:

$$\epsilon'_\theta(x_t | c) = \epsilon_\theta(x_t | c) + (w - 1) \cdot (\epsilon_\theta(x_t | c) - \epsilon_\theta(x_t)), \quad (2)$$

where increasing the guidance scale $w > 1$ amplifies the effect of the condition during sampling. CFG poses limitations in transfer settings: The unconditional noise estimator is prone to underfitting due to joint training under limited target training data (Chen et al. 2023). Further, CFG often steers generations toward out-of-distribution regions in the target domain (Fig. 2 (b)), and it relies on conditionally labeled data, which may be unavailable in some domains (Zhong et al. 2025).

- **Domain Guidance (DoG)** (Zhong et al. 2025) offers a stronger alternative in transfer learning by using the unconditional source model as the marginal noise estimator:

$$\epsilon'_\theta(x_t | c, \mathcal{D}^T) = \epsilon_\theta(x_t | c, \mathcal{D}^T) + (w - 1) \cdot (\epsilon_\theta(x_t | c, \mathcal{D}^T) - \epsilon_{\theta_0}(x_t)), \quad (3)$$

where $\epsilon_\theta(x_t | c, \mathcal{D}^T)$ is the fine-tuned target model’s class-conditional prediction and $\epsilon_{\theta_0}(x_t)$ is the unconditional one of the source model. The source model, having been trained on rich data, provides a stronger reference point than CFG and further improves target domain alignment (Zhong et al. 2025) (Fig. 2 (c)). Like CFG, however, DoG requires two forward passes during sampling.

- **Model Guidance (MG)** (Tang et al. 2025) removes the need for CFG-style computation during sampling by incorporating its effect directly into the training objective. The model is trained to match a guidance-enhanced noise target:

$$\mathcal{L}_{\text{MG}} = \mathbb{E}_{t, (x_0, c), \epsilon} \|\epsilon_\theta(x_t | c) - \epsilon'\|^2, \quad (4)$$

$$\epsilon' = \epsilon + (w - 1) \cdot \text{sg}(\epsilon_\theta(x_t | c) - \epsilon_\theta(x_t)),$$

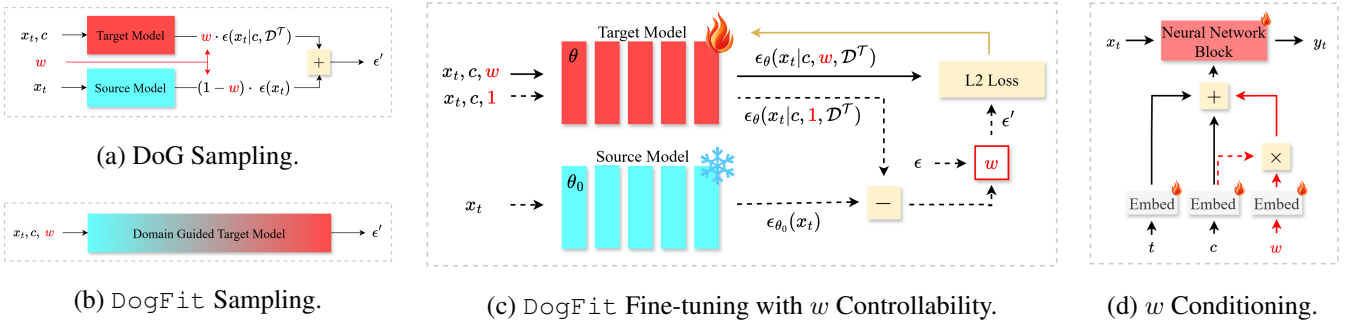


Figure 3: Illustration of DogFit during training and sampling : (a–b) DogFit internalizes guidance behavior, removing the need for inference-time double forward passes. (c) During training, the guidance value is treated as an input, allowing inference-time control. The simple case of our method, with fixed guidance, simply requires removing the w and $\mathbf{1}$ from the target model conditions. (d) w is embedded it as an extra input during fine-tuning, allowing inference-time control. (*) Dashed lines denote paths that do not propagate gradients.

where $\text{sg}(\cdot)$ denotes the stop-gradient operator and ϵ' marks the new noise target. While MG eliminates sampling-time overhead of test-time guidance, it inherits CFG’s limitations in transfer learning due to the underfitting of the unconditional noise estimator. Further, it lacks a clear mechanism for allowing diversity-fidelity control at test time—a crucial principle in diffusion guidance.



Domain Guided Fine-Tuning

We propose DogFit, a training-time guidance mechanism for diffusion transfer learning that integrates a domain-aware guidance direction directly into the loss during fine-tuning. The marginal estimate of DogFit is derived from the unconditional source model (Fig.3 (a-b)). It modifies the training loss as:

$$\mathcal{L}_{\text{DogFit}} = \mathbb{E}_{t, (x_0, c), \epsilon} \left\| \epsilon_{\theta}(x_t | c, \mathcal{D}^{\mathcal{T}}) - \epsilon' \right\|^2, \quad (5)$$

$$\epsilon' = \epsilon + (w - 1) \cdot \text{sg}(\epsilon_{\theta}(x_t | c, \mathcal{D}^{\mathcal{T}}) - \epsilon_{\theta_0}(x_t)).$$

The training architecture is illustrated in Fig. 3(c). The training algorithm is shown in Appx. The rest of this subsection provides theoretical insights motivating the design of DogFit (full statements and proofs in Appx.)

Proposition 1. *Suppose a model is trained using the DogFit objective with controllable guidance strength w (Eq. 6), and the following assumptions hold: (i) the model approximately recovers the true noise when no guidance is applied, and (ii) its predictions vary linearly with w . Then, for any value of w , the model replicates the effect of applying DoG at sampling time.*

Proposition 2. *DogFit is equivalent to implicitly applying a domain alignment component to MG’s training loss, benefiting from the class-conditional guidance of MG while reducing the risk of out-of-distribution generation.*

This means that ϵ_{θ_0} provides a strong and stable marginal noise estimate not only as an inference-time signal, but also during fine-tuning. Further, the domain alignment term, independent of class conditioning, pulls samples toward the

core of the target data manifold, rendering DogFit effective even in the unconditional setting. In summary, it combines the strengths of previous guidance mechanisms in transfer learning into a single framework: it inherits the fast, single-pass sampling of MG and the robust marginal noise estimator of DoG. W

Incorporating Controllability

A crucial feature of guidance is its controllability. To enable efficient fidelity–diversity trade-offs at test time, we introduce a lightweight conditioning mechanism to the model and treat w as an additional input condition during fine-tuning. The training objective with added control is:

$$\mathcal{L}_{\text{DogFit}} = \mathbb{E}_{t, (x_0, c, w), \epsilon} \left\| \epsilon_{\theta}(x_t | c, w, \mathcal{D}^{\mathcal{T}}) - \epsilon' \right\|^2, \quad (6)$$

$$\epsilon' = \epsilon + (w - 1) \cdot \text{sg}(\epsilon_{\theta}(x_t | c, \mathbf{1}, \mathcal{D}^{\mathcal{T}}) - \epsilon_{\theta_0}(x_t)),$$

where $\epsilon_{\theta}(x_t | c, \mathbf{1}, \mathcal{D}^{\mathcal{T}})$ is the unguided class-conditional prediction. During training, the model must learn to operate across a range of guidance strengths to support controllable fidelity–diversity trade-offs at inference, while still preserving stable behavior in the unguided setting. Our initial experiments revealed that a simple uniform sampling of w during training can reduce diversity and destabilize generation, even at lower guidance levels due to excessive exposure to high w . We sample w from a shifted exponential decaying distribution (SEDD; see distribution CDF in Appx.):

$$w = 1 + z, \quad z \sim \mathcal{P}(z), \quad (7)$$

$$\mathcal{P}(z) = \lambda e^{-\lambda z}, \quad z \geq 0, \quad (8)$$

where λ controls the decay rate. This distribution favors smaller guidance strengths while occasionally introducing larger values, enabling guidance robustness without destabilizing training. As a result, the model generalizes well across the guidance spectrum and supports dynamic controllability at inference (Fig. 5; see comparison with uniform scheduling in Appx.). The next key question is *how to actually incorporate w into the model?*

In conditional diffusion models, the final condition embedding is typically formed by summing the label c and

	Metric	Method	Unlabeled	Labeled						Sampling Cost	
			FFHQ	ArtBench	Caltech	CUB-Birds	Food	Stanford-Cars	Avg.	Passes	TFLOPS
DiT/XL-2	FID ↓	Fine-tuning	15.94	23.36	30.02	9.35	16.75	16.24	19.14	x1	366.14
		+ CFG (Ho and Salimans 2022)	–	20.83	24.07	5.03	11.77	10.60	14.46	x2	732.28
		+ DoG (Zhong et al. 2025)	13.87	17.30	23.76	3.65	10.97	<u>9.77</u>	13.09	x2	732.28
		MG (Tang et al. 2025)	–	19.91	23.71	4.85	11.13	11.03	14.13	x1	366.14
		DogFit	10.48	16.32	21.68	<u>3.69</u>	<u>10.64</u>	9.35	12.34	x1	366.14
	DogFit + Control	<u>13.03</u>	<u>16.98</u>	<u>21.98</u>	<u>3.69</u>	10.44	10.05	<u>12.63</u>	x1	366.14	
	FD _{DINOv2} ↓	Fine-tuning	461.45	360.77	529.85	428.21	610.31	378.11	461.45	x1	366.14
		+ CFG (Ho and Salimans 2022)	–	314.32	401.96	200.92	410.48	227.46	311.03	x2	732.28
		+ DoG (Zhong et al. 2025)	273.93	<u>266.25</u>	<u>377.49</u>	135.74	314.16	132.91	245.31	x2	732.28
		MG (Tang et al. 2025)	–	299.06	409.20	220.40	379.39	255.88	312.78	x1	366.14
DogFit		282.32	269.06	377.15	<u>143.42</u>	293.24	147.20	<u>246.01</u>	x1	366.14	
DogFit + Control	<u>274.67</u>	261.72	378.86	144.39	<u>314.12</u>	<u>141.08</u>	248.03	x1	366.14		
SiT/XL-2	FID ↓	Fine-tuning	7.63	9.66	26.10	4.92	<u>7.76</u>	10.53	11.79	x1	454.01
		+ CFG (Ho and Salimans 2022)	-	9.28	23.21	3.49	7.95	<u>9.71</u>	10.73	x2	1083.77
		+ DoG (Zhong et al. 2025)	7.63	11.22	23.53	3.39	7.95	<u>9.71</u>	11.16	x2	1083.77
		MG (Tang et al. 2025)	-	9.64	23.10	3.60	<u>6.84</u>	8.62	10.36	x1	454.01
		DogFit	12.44	9.62	23.45	3.52	7.85	10.05	10.91	x1	454.01
	DogFit + Control	<u>10.8</u>	9.03	23.15	3.59	6.52	10.10	<u>10.48</u>	x1	454.01	
	FD _{DINOv2} ↓	Fine-tuning	335.15	271.92	519.54	405.07	522.47	283.29	400.46	x1	454.01
		+ CFG (Ho and Salimans 2022)	-	236.13	406.63	203.47	368.26	190.24	280.94	x2	1083.77
		+ DoG (Zhong et al. 2025)	335.15	215.12	387.89	<u>160.85</u>	<u>298.65</u>	139.09	<u>240.32</u>	x2	1083.77
		MG (Tang et al. 2025)	-	232.17	418.86	229.32	359.90	203.23	288.70	x1	454.01
DogFit		278.10	<u>222.20</u>	403.44	181.48	<u>296.49</u>	<u>159.83</u>	252.29	x1	454.01	
DogFit + Control	<u>319.16</u>	230.23	<u>399.20</u>	152.50	234.98	183.41	240.06	x1	454.01		

Table 1: FID and FD_{DINOv2} performance of DogFit against SOTA methods using DiT/XL-2 and SiT/XL-2 backbones. Their sampling costs are also shown in terms of forward passes and TFLOPs.



Figure 4: Qualitative comparison of guidance mechanisms on DiT-XL/2 (guidance scale 1.5). ×: not applicable.

time-step t embeddings. Therefore, a natural approach to add w is to embed it and sum it with the other existing embeddings. However, we saw that even slight distributional shifts and directional changes can destabilize training and disrupt the pretrained features. To avoid this, we use w as a label modulator: we embed it as a scalar, multiply it with

a detached label c embedding, and add the resulting modulation vector to the condition embedding. This allows w to control the influence of the label without altering its semantic direction, preserving the integrity of the pretrained embedding space and ensuring stable guidance conditioning. For the unconditional case, we use the same formulation while keeping c as a fixed zero vector.

Guidance Scheduling Mechanisms

Inspired by test-time guidance scheduling for improved generation quality (Sadat et al. 2023; Kynkäänniemi et al. 2024), we investigate the optimal timing and placement of training-time guidance using two simple yet effective strategies. First, we introduce a *late-start* mechanism that delays the injection of guidance until iteration $s > \tau_s$, avoiding noisy updates and unstable gradients in the early phases of training. This is particularly beneficial in conditional settings where class embeddings are reinitialized to accommodate mismatched source and target label spaces. By deferring guidance, the model benefits from more stable target representations and condition embeddings, resulting in higher-fidelity updates. Second, we introduce a *cut-off* strategy that disables guidance at higher noise levels ($t > \tau_c$), concentrating domain supervision on the later denoising stages where adaptation to target-specific details is most effective (Choi et al. 2022). This design preserves source-driven diversity in the early denoising steps and prevents the model from over-relying on the target domain to shape the global structure

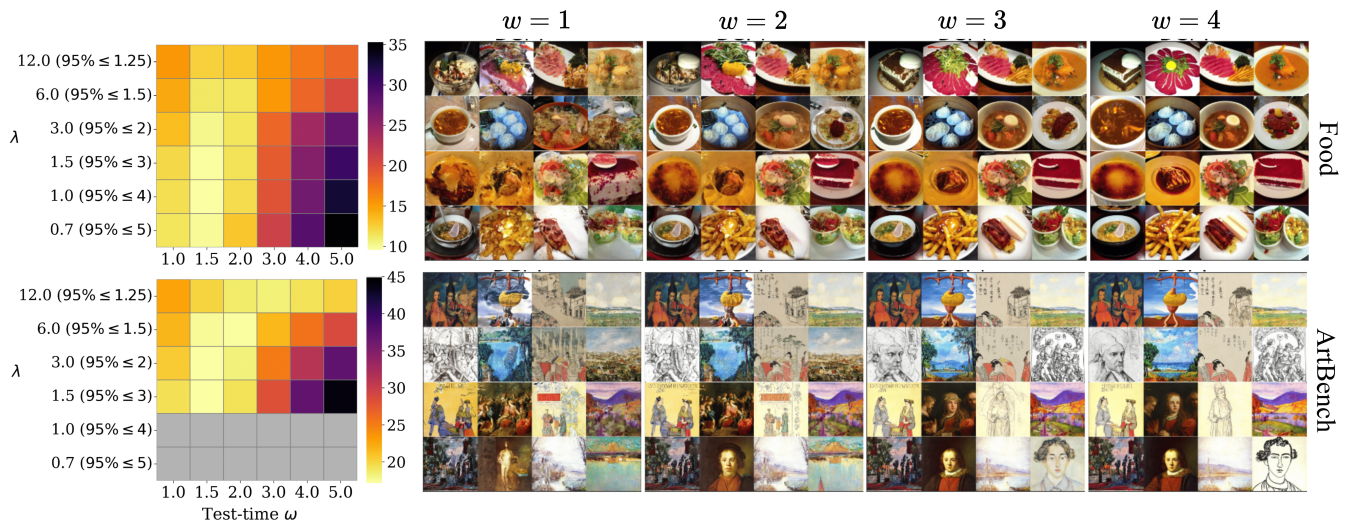


Figure 5: Effect of controllable guidance at test time for the Food and ArtBench domains. (Left) FID behavior across test-time w s with different training-time λ s. (Right) Corresponding generated samples for fixed $\lambda = 3$ (95% of sampled w values in $[1, 2]$), across varying test-time w . Gray cells indicate extreme FID values (≈ 350) resulting from collapsed generations.

of the image. This becomes crucial when source and target domains share similar structural priors (e.g. FFHQ faces).

Results and Discussion

Setup. DogFit is validated on six challenging datasets with diverse domain characteristics and label availability for a comprehensive assessment: Food101 (Bossard, Guillaumin, and Van Gool 2014), Caltech101 (Griffin et al. 2007), CUB-200-201 (Wah et al. 2011), ArtBench10 (Liao et al. 2022), Stanford-Cars (Krause et al. 2013), and FFHQ256 (Karras, Laine, and Aila 2019). These datasets range from fine-grained species (Wah et al. 2011) to abstract art-styles (Liao et al. 2022) and face generation (Karras, Laine, and Aila 2019), covering a variety of distribution shifts in appearance, texture, and structure. We compare DogFit to standard fine-tuning, CFG, DoG, and MG. All methods are applied on DiT-XL/2 (Peebles and Xie 2023) and SiT-XL/2 (Ma et al. 2024) backbones pre-trained on ImageNet at 256×256 resolution for 7M steps with Fréchet Inception Distance (FID) (Heusel et al. 2017) scores of 2.27 (DiT) and 2.06 (SiT). We generate 10,000 images using 50 sampling steps (Peebles and Xie 2023; Xie et al. 2023), fixing guidance strength to 1.5 for fair comparison, and fine-tune for 24,000 training steps (Zhong et al. 2025) with batch size of 32 on 2 A100 GPUs for 5 hours. We calculate FID and FD_{DINOv2} (Stein et al. 2023) between the generated images and the full datasets to evaluate the generation quality. Further, we compute Precision and Recall (Kynkäänniemi et al. 2019) for analyzing fidelity and diversity.

Comparison with State-of-the-art Methods

Tab.?? summarizes our main quantitative findings. DogFit consistently performs comparatively or superior to prior methods in both FID and FD_{DINOv2} , while maintaining the efficiency of one-pass sampling. Unlike CFG and MG,

DogFit remains effective in unconditional settings like FFHQ due to its class-agnostic domain-alignment direction. On SiT, CFG and MG slightly outperform DogFit in FID, but DogFit outperforms both CFG and MG on FD_{DINOv2} , underscoring the value of utilizing diverse metrics for comprehensive evaluation. Importantly, equipping DogFit with controllable guidance introduces no performance degradation while increasing the parameter count by only 1.33 million parameters (less than 2% of the initial network parameters), leaving no notable impact on sampling TFLOPS. Additional results on Precision and Recall are provided in Appx. Fig. 4 presents a visual comparison of generated samples across target domains on DiT. Guidance-based methods consistently outperform naïve fine-tuning by producing more realistic and coherent images. DogFit generates sharp, domain-relevant details on par with or better looking than DoG, while avoiding off-distribution artifacts occasionally seen with CFG and MG (e.g., distorted faces or tires). SiT qualitative results are provided in Appx.

Ablation Studies

Controllable Guidance We study the effect of λ for sampling the guidance scalar w from the SED during training (Eq. 8). As shown in Fig. 5 (left), sparse exposure to higher guidance is sufficient for generalization and achieving a diversity-fidelity tradeoff. In contrast, excessive exposure to large guidance can harm the model’s ability to retain pretrained features, leading to instability and collapsed generations. Based on these findings, we adopt $\lambda = 3$ (95% of sampled w s in $[1, 2]$) for all experiments. Fig. 5 (right) illustrates how varying guidance strength at test time effectively modulates the trade-off between fidelity and diversity, increasing sample quality while reducing variation with higher guidance values (more analysis in Appx).

Guidance Scheduling. We analyze the impact of late-start

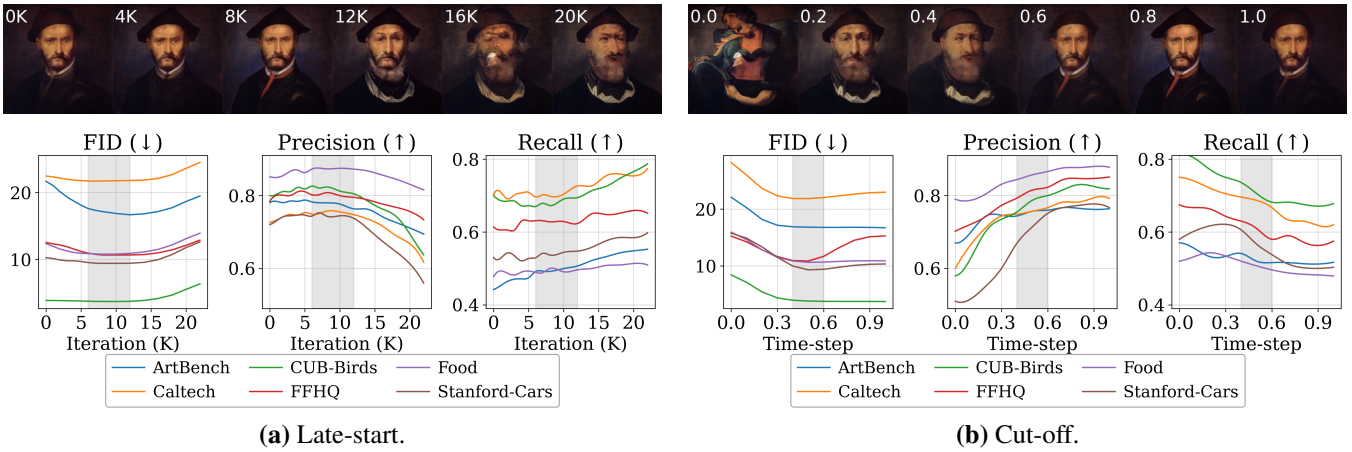


Figure 6: Ablation study on guidance schedules in DogFit. (a) Varying the late-start threshold τ_s to control when guidance begins. (b) Varying the cut-off threshold τ_c to restrict guidance to later denoising steps. Performed using FID on DiT-XL/2.

# Steps	Food FID↓		Art FID↓	
	MG	DogFit	MG	DogFit
10	60.60	57.91	108.26	88.84
25	21.13	18.97	39.80	29.11
50	11.13	10.64	19.91	16.32
100	7.60	8.09	13.38	12.70

Table 2: Varying the number of sampling steps for MG and DogFit.

DiT-XL/2 Variant	FID↓		Train Params (M)
	Food	Art	
DogFit	10.64	16.32	675.42 (100%)
+ DiffFit	11.86	15.80	0.75 (0.11%)

Table 3: Using DogFit with PEFT.

and cut-off on generation quality and diversity. Fig. 6(a) shows how varying the late-start threshold τ_s impacts FID, Precision, and Recall. Delaying guidance improves FID and especially Precision at first, as early stabilization allows formation of more accurate directional cues. However, setting τ_s too high leaves insufficient time for the model to internalize guidance, reducing it to naïve fine-tuning and lowering precision. We set $\tau_s = 12k$ for FID and $\tau_s = 6k$ for FD_{DINOv2} in all experiments. Fig. 6(b) shows the effect of cut-off threshold τ_c on FID, Precision, and Recall. Delaying guidance to later denoising steps enhances diversity, particularly for target datasets with strong global structural similarity to the source domain, such as FFHQ, Cars, and Caltech. However, setting τ_c too low limits exposure to guidance, again reducing the model to naïve fine-tuning. While the optimal τ_c may depend on the source–target similarity, we use $\tau_c = 0.5$ for FID and $\tau_c = 1$ for FD_{DINOv2} in our experiments ($t \in [0, 1]$). See FD_{DINOv2} analysis in Appx.

Domain-guided Parameter-efficient Fine-tuning. We demonstrate that DogFit is fully compatible with DiffFit, a leading PEFT method for DiT models (Xie et al. 2023).

As shown in Tab.3, combining the two yields high-quality generations with lower cost in both training and test-time. This highlights DogFit’s practicality as a simple drop-in enhancement for efficient fine-tuning mechanisms.

Sampling Steps. Tab.2 reports the effect of varying the number of sampling steps during generation. DogFit outperforms MG in nearly all settings, with especially notable gains at lower step counts. This underscores the effectiveness of DogFit’s target alignment in low-resource scenarios where fast sampling is critical.

Conclusion

We introduce DogFit, a training-time guidance strategy for diffusion model transfer learning. It eliminates the high sampling-time cost of test-time guidance while preserving strong generalization behavior and controllability. DogFit leverages the pre-trained source model to inject high quality, domain-aligned guidance signals directly into the fine-tuning loss, and relies on a lightweight conditioning mechanism for inference fidelity–diversity adjustments. Our training-time guidance scheduling strategies further enhance training stability and generation quality. Extensive experiments across diverse target datasets and models show that DogFit can surpass the performance and efficiency of SOTA guidance methods, establishing it as a practical solution for scalable diffusion model transfer.

Limitations and Future Work. While effective, the proposed guidance scheduling strategies rely on manually chosen, fixed thresholds. Future work explores adaptive or data-driven approaches that respond to training dynamics or domain-specific properties. Moreover, extension of DogFit to broader settings, i.e., text-to-image, audio, and video generation remains an exciting direction.

Acknowledgments

This research was supported by the Natural Sciences and Engineering Research Council of Canada, and the Digital Research Alliance of Canada.

References

- Bossard, L.; Guillaumin, M.; and Van Gool, L. 2014. Food-101—mining discriminative components with random forests. In *Computer vision—ECCV 2014: 13th European conference, Zurich, Switzerland, September 6–12, 2014, proceedings, part VI 13*, 446–461. Springer.
- Cao, Y.; and Gong, S. 2024. Few-shot image generation by conditional relaxing diffusion inversion. In *European Conference on Computer Vision*, 20–37. Springer.
- Chen, H.; Jiang, K.; Zheng, K.; Chen, J.; Su, H.; and Zhu, J. 2025. Visual Generation Without Guidance. *arXiv preprint arXiv:2501.15420*.
- Chen, M.; Huang, K.; Zhao, T.; and Wang, M. 2023. Score approximation, estimation and distribution recovery of diffusion models on low-dimensional data. In *International Conference on Machine Learning*, 4672–4712. PMLR.
- Choi, J.; Lee, J.; Shin, C.; Kim, S.; Kim, H.; and Yoon, S. 2022. Perception prioritized training of diffusion models. In *Proceedings of the IEEE/CVF Conference on Computer Vision and Pattern Recognition*, 11472–11481.
- Deja, K.; Kuzina, A.; Trzcinski, T.; and Tomczak, J. 2022. On analyzing generative and denoising capabilities of diffusion-based deep generative models. *Advances in Neural Information Processing Systems*, 35: 26218–26229.
- Dhariwal, P.; and Nichol, A. 2021. Diffusion models beat gans on image synthesis. *Advances in neural information processing systems*, 34: 8780–8794.
- Griffin, G.; Holub, A.; Perona, P.; et al. 2007. Caltech-256 object category dataset. Technical report, Technical Report 7694, California Institute of Technology Pasadena.
- Gupta, A.; Yu, L.; Sohn, K.; Gu, X.; Hahn, M.; Li, F.-F.; Essa, I.; Jiang, L.; and Lezama, J. 2024. Photorealistic video generation with diffusion models. In *European Conference on Computer Vision*, 393–411. Springer.
- Helber, P.; Bischke, B.; Dengel, A.; and Borth, D. 2019. Eurosat: A novel dataset and deep learning benchmark for land use and land cover classification. *IEEE Journal of Selected Topics in Applied Earth Observations and Remote Sensing*.
- Heusel, M.; Ramsauer, H.; Unterthiner, T.; Nessler, B.; and Hochreiter, S. 2017. Gans trained by a two time-scale update rule converge to a local nash equilibrium. *Advances in neural information processing systems*, 30.
- Ho, J.; Jain, A.; and Abbeel, P. 2020. Denoising diffusion probabilistic models. *Advances in neural information processing systems*, 33: 6840–6851.
- Ho, J.; and Salimans, T. 2022. Classifier-free diffusion guidance. *arXiv preprint arXiv:2207.12598*.
- Ho, J.; Salimans, T.; Gritsenko, A.; Chan, W.; Norouzi, M.; and Fleet, D. J. 2022. Video diffusion models. *Advances in Neural Information Processing Systems*, 35: 8633–8646.
- Hsiao, Y.-T.; Khodadadeh, S.; Duarte, K.; Lin, W.-A.; Qu, H.; Kwon, M.; and Kalarot, R. 2024. Plug-and-play diffusion distillation. In *Proceedings of the IEEE/CVF Conference on Computer Vision and Pattern Recognition*, 13743–13752.
- Hu, E. J.; Shen, Y.; Wallis, P.; Allen-Zhu, Z.; Li, Y.; Wang, S.; Wang, L.; Chen, W.; et al. 2022. Lora: Low-rank adaptation of large language models. *ICLR*, 1(2): 3.
- Hur, J.; Choi, J.; Han, G.; Lee, D.-J.; and Kim, J. 2024. Expanding expressiveness of diffusion models with limited data via self-distillation based fine-tuning. In *Proceedings of the IEEE/CVF Winter Conference on Applications of Computer Vision*, 5028–5037.
- Jensen, C. P.; and Sadat, S. 2025. Efficient Distillation of Classifier-Free Guidance using Adapters. *arXiv preprint arXiv:2503.07274*.
- Karras, T.; Aittala, M.; Kynkäänniemi, T.; Lehtinen, J.; Aila, T.; and Laine, S. 2024. Guiding a diffusion model with a bad version of itself. *Advances in Neural Information Processing Systems*, 37: 52996–53021.
- Karras, T.; Laine, S.; and Aila, T. 2019. A style-based generator architecture for generative adversarial networks. In *Proceedings of the IEEE/CVF conference on computer vision and pattern recognition*, 4401–4410.
- Kawar, B.; Zada, S.; Lang, O.; Tov, O.; Chang, H.; Dekel, T.; Mosseri, I.; and Irani, M. 2023. Imagic: Text-based real image editing with diffusion models. In *Proceedings of the IEEE/CVF conference on computer vision and pattern recognition*, 6007–6017.
- Krause, J.; Stark, M.; Deng, J.; and Fei-Fei, L. 2013. 3d object representations for fine-grained categorization. In *Proceedings of the IEEE international conference on computer vision workshops*, 554–561.
- Kynkäänniemi, T.; Aittala, M.; Karras, T.; Laine, S.; Aila, T.; and Lehtinen, J. 2024. Applying guidance in a limited interval improves sample and distribution quality in diffusion models. *arXiv preprint arXiv:2404.07724*.
- Kynkäänniemi, T.; Karras, T.; Laine, S.; Lehtinen, J.; and Aila, T. 2019. Improved precision and recall metric for assessing generative models. *Advances in neural information processing systems*, 32.
- Liao, P.; Li, X.; Liu, X.; and Keutzer, K. 2022. The art-bench dataset: Benchmarking generative models with artworks. *arXiv preprint arXiv:2206.11404*.
- Lu, C.; Zhou, Y.; Bao, F.; Chen, J.; Li, C.; and Zhu, J. 2022. Dpm-solver: A fast ode solver for diffusion probabilistic model sampling in around 10 steps. *Advances in Neural Information Processing Systems*, 35: 5775–5787.
- Ma, N.; Goldstein, M.; Albergo, M. S.; Boffi, N. M.; Vanden-Eijnden, E.; and Xie, S. 2024. Sit: Exploring flow and diffusion-based generative models with scalable interpolant transformers. In *European Conference on Computer Vision*, 23–40. Springer.
- Meng, C.; He, Y.; Song, Y.; Song, J.; Wu, J.; Zhu, J.-Y.; and Ermon, S. 2021. Sdedit: Guided image synthesis and editing with stochastic differential equations. *arXiv preprint arXiv:2108.01073*.
- Moon, T.; Choi, M.; Lee, G.; Ha, J.-W.; and Lee, J. 2022. Fine-tuning diffusion models with limited data. In *NeurIPS 2022 Workshop on Score-Based Methods*.

- Nichol, A.; Dhariwal, P.; Ramesh, A.; Shyam, P.; Mishkin, P.; McGrew, B.; Sutskever, I.; and Chen, M. 2021. Glide: Towards photorealistic image generation and editing with text-guided diffusion models. *arXiv preprint arXiv:2112.10741*.
- Ouyang, Y.; Xie, L.; Zha, H.; and Cheng, G. 2024. Transfer Learning for Diffusion Models. *arXiv preprint arXiv:2405.16876*.
- Peebles, W.; and Xie, S. 2023. Scalable diffusion models with transformers. In *Proceedings of the IEEE/CVF international conference on computer vision*, 4195–4205.
- Phunyaphibarn, P.; Lee, P. Y.; Kim, J.; and Sung, M. 2025. Unconditional Priors Matter! Improving Conditional Generation of Fine-Tuned Diffusion Models. *arXiv preprint arXiv:2503.20240*.
- Podell, D.; English, Z.; Lacey, K.; Blattmann, A.; Dockhorn, T.; Müller, J.; Penna, J.; and Rombach, R. 2023. Sdxl: Improving latent diffusion models for high-resolution image synthesis. *arXiv preprint arXiv:2307.01952*.
- Rombach, R.; Blattmann, A.; Lorenz, D.; Esser, P.; and Ommer, B. 2022. High-resolution image synthesis with latent diffusion models. In *Proceedings of the IEEE/CVF conference on computer vision and pattern recognition*, 10684–10695.
- Ruiz, N.; Li, Y.; Jampani, V.; Pritch, Y.; Rubinstein, M.; and Aberman, K. 2023. Dreambooth: Fine tuning text-to-image diffusion models for subject-driven generation. In *Proceedings of the IEEE/CVF conference on computer vision and pattern recognition*, 22500–22510.
- Sadat, S.; Buhmann, J.; Bradley, D.; Hilliges, O.; and Weber, R. M. 2023. CADs: Unleashing the diversity of diffusion models through condition-annealed sampling. *arXiv preprint arXiv:2310.17347*.
- Salimans, T.; and Ho, J. 2022. Progressive distillation for fast sampling of diffusion models. *arXiv preprint arXiv:2202.00512*.
- Shen, H.; Zhang, J.; Xiong, B.; Hu, R.; Chen, S.; Wan, Z.; Wang, X.; Zhang, Y.; Gong, Z.; Bao, G.; et al. 2025. Efficient Diffusion Models: A Survey. *arXiv preprint arXiv:2502.06805*.
- Sohl-Dickstein, J.; Weiss, E.; Maheswaranathan, N.; and Ganguli, S. 2015. Deep unsupervised learning using nonequilibrium thermodynamics. In *International conference on machine learning*, 2256–2265. pmlr.
- Song, J.; Meng, C.; and Ermon, S. 2020. Denoising diffusion implicit models. *arXiv preprint arXiv:2010.02502*.
- Stein, G.; Cresswell, J.; Hosseinzadeh, R.; Sui, Y.; Ross, B.; Vilecroze, V.; Liu, Z.; Caterini, A. L.; Taylor, E.; and Loaiza-Ganem, G. 2023. Exposing flaws of generative model evaluation metrics and their unfair treatment of diffusion models. *Advances in Neural Information Processing Systems*, 36: 3732–3784.
- Tang, Z.; Bao, J.; Chen, D.; and Guo, B. 2025. Diffusion Models without Classifier-free Guidance. *arXiv preprint arXiv:2502.12154*.
- Wah, C.; Branson, S.; Welinder, P.; Perona, P.; and Belongie, S. 2011. The Caltech-UCSD Birds-200-2011 Dataset. Technical Report CNS-TR-2011-001, California Institute of Technology, Pasadena, CA, USA.
- Wang, X.; Lin, B.; Liu, D.; Chen, Y.-C.; and Xu, C. 2024. Bridging data gaps in diffusion models with adversarial noise-based transfer learning. In *Forty-first International Conference on Machine Learning*.
- Weiss, K.; Khoshgoftaar, T. M.; and Wang, D. 2016. A survey of transfer learning. *Journal of Big data*, 3: 1–40.
- Xie, E.; Yao, L.; Shi, H.; Liu, Z.; Zhou, D.; Liu, Z.; Li, J.; and Li, Z. 2023. Diffit: Unlocking transferability of large diffusion models via simple parameter-efficient fine-tuning. In *Proceedings of the IEEE/CVF International Conference on Computer Vision*, 4230–4239.
- Yin, T.; Gharbi, M.; Zhang, R.; Shechtman, E.; Durand, F.; Freeman, W. T.; and Park, T. 2024. One-step diffusion with distribution matching distillation. In *Proceedings of the IEEE/CVF conference on computer vision and pattern recognition*, 6613–6623.
- Zheng, C.; and Lan, Y. 2023. Characteristic guidance: Non-linear correction for diffusion model at large guidance scale. *arXiv preprint arXiv:2312.07586*.
- Zheng, K.; Lu, C.; Chen, J.; and Zhu, J. 2023. Improved techniques for maximum likelihood estimation for diffusion odes. In *International Conference on Machine Learning*, 42363–42389. PMLR.
- Zhong, J.; Guo, X.; Dong, J.; and Long, M. 2024. Diffusion tuning: Transferring diffusion models via chain of forgetting. *arXiv preprint arXiv:2406.00773*.
- Zhong, J.; Zhang, X.; Wang, J.; and Long, M. 2025. Domain guidance: A simple transfer approach for a pre-trained diffusion model. *arXiv preprint arXiv:2504.01521*.
- Zhou, Z.; Chen, D.; Wang, C.; Chen, C.; and Lyu, S. 2025. DICE: Distilling Classifier-Free Guidance into Text Embeddings. *arXiv preprint arXiv:2502.03726*.
- Zhu, J.; Ma, H.; Chen, J.; and Yuan, J. 2022. Few-shot image generation with diffusion models. *arXiv preprint arXiv:2211.03264*.

Appendix

Additional Methodology Explanations

DogFit Algorithm

Algorithm 1 summarizes the training loop of DogFit with controllability through guidance conditioning and the scheduling strategies.

Algorithm 1: DogFit training with Controllable Guidance and Scheduling

Require: Target dataset $\{\mathcal{D}^T\}$, noise schedule $\bar{\alpha}$, fixed source model ϵ_{θ_0} , training model ϵ_θ initialized by ϵ_{θ_0} , guidance cut-off τ_c , late-start step τ_s .

- 1: **for** training step $s = 1$ to S **do**
- 2: Sample target data $(x_0, c) \sim \{\mathcal{D}^T\}$
- 3: Sample noise $\epsilon \sim \mathcal{N}(0, 1)$ and time-step $t \sim \mathcal{U}(0, 1)$
- 4: Sample guidance strength $w = 1 + z$, $z \sim \mathcal{P}(z)$
- 5: Add noise: $x_t = \sqrt{\bar{\alpha}_t}x_0 + \sqrt{1 - \bar{\alpha}_t} \cdot \epsilon$
- 6: **if** $s > \tau_s$ **and** $t < \tau_c$ **then**
- 7: Compute guided target:
 $\epsilon' = \epsilon + (w - 1) \cdot \text{sg}(\epsilon_\theta(x_t | c, \mathbf{1}, \mathcal{D}^T) - \epsilon_{\theta_0}(x_t))$
- 8: **else**
- 9: $\epsilon' = \epsilon$
- 10: **end if**
- 11: Compute loss: $\mathcal{L}_{\text{DogFit}} = \|\epsilon_\theta(x_t | c, w, \mathcal{D}^T) - \epsilon'\|^2$
- 12: Backpropagate and update: $\theta = \theta - \eta \nabla_\theta \mathcal{L}_{\text{DogFit}}$
- 13: **end for**

CDF of Sampled Guidance Strengths

Fig. 7 visualizes the Cumulative Distribution Function (CDF) of w s sampled during training from the shifted exponentially decaying distribution (SEDD) in Equation 8. Larger values of λ concentrate the sampling mass closer to $w = 1$, limiting exposure to higher guidance values during training. This design ensures that the model primarily learns under weak to moderate guidance, while still sparsely encountering stronger guidance values.

Theoretical Insights into DogFit

In this section, we motivate the shift from using the marginal target noise estimate to the marginal source estimate in transfer learning. We discuss the benefits of this shift, and justify our method of applying it in the fine-tuning process. Then we show that under mild assumptions, DogFit learns to internalize DoG’s behaviour. Further, we conjecture that DogFit is an extension of MG, with an added domain alignment term.

General Assumptions. We assume that both the pretrained source model ϵ_{θ_0} and the fine-tuned model ϵ_θ share the same architecture and noise schedule (α_t), and are trained to approximate the same family of score functions under a common sampling procedure.

Guidance via Unconditional Source Prior The guidance signal in CFG is originally created via the target domain conditional posterior $p_\theta(c | x_t, \mathcal{D}^T)$ to encourage sample

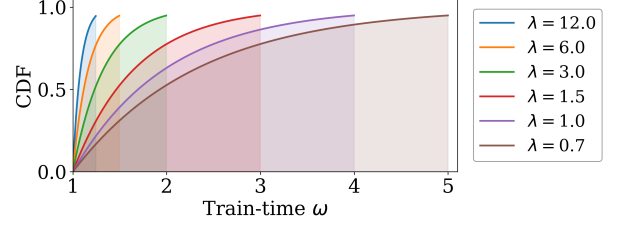


Figure 7: The CDF of sampled guidance strengths w during training for various λ values using SEDD. The shaded region covers 95% of the samples.

fidelity and strong class-conditional alignment in the target domain. By Bayes’ rule:

$$p_\theta(c | x_t, \mathcal{D}^T) = \frac{p_\theta(x_t | c, \mathcal{D}^T) \cdot p_\theta(c | \mathcal{D}^T)}{p_\theta(x_t | \mathcal{D}^T)}, \quad (9)$$

or equivalently, in the log form:

$$\begin{aligned} \log p_\theta(c | x_t, \mathcal{D}^T) &= & (10) \\ \log p_\theta(x_t | c, \mathcal{D}^T) - \log p_\theta(x_t | \mathcal{D}^T) + \log p_\theta(c | \mathcal{D}^T). \end{aligned}$$

We consider the score functions (gradients of log-densities):

$$\begin{aligned} \nabla_{x_t} \log p_\theta(c | x_t, \mathcal{D}^T) &= & (11) \\ \nabla_{x_t} \log p_\theta(x_t | c, \mathcal{D}^T) - \nabla_{x_t} \log p_\theta(x_t | \mathcal{D}^T), \end{aligned}$$

which are approximated by diffusion models:

$$\nabla_{x_t} \log p_\theta(x_t | c, \mathcal{D}^T) \approx -\frac{1}{\sigma_t} \epsilon_\theta(x_t | c, \mathcal{D}^T), \quad (12)$$

$$\nabla_{x_t} \log p_\theta(x_t | \mathcal{D}^T) \approx -\frac{1}{\sigma_t} \epsilon_{\theta_0}(x_t | \mathcal{D}^T). \quad (13)$$

Traditionally, CFG estimates both the class-conditional (Equation 12) and the marginal (Equation 13) noises with the same diffusion model. With enough data in the target domain, the class-conditional noise can be well estimated during fine-tuning via $\epsilon_\theta(x_t | c, \mathcal{D}^T)$. However, learning the target noise estimator $\epsilon_\theta(x_t | \mathcal{D}^T)$ faces the risk of undertraining due to only being trained on a small portion of the small target dataset. Since the source model is usually trained on large, diverse datasets, it likely captures a good approximation of the general image manifold. Furthermore, it has been shown that diffusion models have generalizability on other data distributions (Deja et al. 2022) and can denoise noisy images from domains other than those they have been trained on (Meng et al. 2021). Therefore, we can assume that the pre-trained source model captures a general enough prior, giving us the ability to approximate the unconditional score using the pre-trained source model, leading to the formulation of DoG:

$$\nabla_{x_t} \log p_\theta(x_t | \mathcal{D}^T) \approx -\frac{1}{\sigma_t} \epsilon_{\theta_0}(x_t). \quad (14)$$

Thus, the posterior score can be approximated as:

$$\nabla_{x_t} \log p_{\theta}(c | x_t, \mathcal{D}^T) \propto -\frac{1}{\sigma_t} (\epsilon_{\theta}(x_t | c, \mathcal{D}^T) - \epsilon_{\theta_0}(x_t)), \quad (15)$$

which exactly matches the offset used in DoG sampling (Zhong et al. 2025). Our method takes a step further from this and applies the same guidance offset online. We train a diffusion model to directly predict this guided score instead of separately learning Equations 12 and 13 in the form of DoG.

Proposition 1. Let $\epsilon_{\theta}(x_t | c, w)$ be the `DogFit` model with controllable guidance trained with the objective:

$$\mathcal{L}_{\text{DogFit}} = \left\| \epsilon_{\theta}(x_t | c, w, \mathcal{D}^T) - (\epsilon + (w - 1) \cdot \Delta(x_t, c, \mathcal{D}^T)) \right\|^2, \quad (16)$$

where $\Delta(x_t, c, \mathcal{D}^T) = \epsilon_{\theta}(x_t | c, w = 1, \mathcal{D}^T) - \epsilon_{\theta_0}(x_t)$ and assume the following conditions hold after convergence:

- (i) When no guidance is applied, the model approximately recovers the true noise ϵ used in training.
- (ii) The model’s prediction varies linearly with the guidance strength w .

Then for any w , the `DogFit` model matches the DoG-guided score used at sampling time:

$$\begin{aligned} \epsilon_{\theta}(x_t | c, w, \mathcal{D}^T) &= \quad (17) \\ \epsilon_{\theta}(x_t | c, \mathcal{D}^T) + (w - 1) \cdot (\epsilon_{\theta}(x_t | c, \mathcal{D}^T) - \epsilon_{\theta_0}(x_t)). \end{aligned}$$

Note on the assumptions: Prior work on CFG has shown that the linearity assumption holds in practice for low to moderate w values (Zheng and Lan 2023). Furthermore, our use of an SED to sample w during training (see Section 3) helps maintain accurate estimation of ϵ in the unconditional setting. Based on this, we conjecture that both assumptions can approximately hold in practice.

Proof sketch. At convergence, the `DogFit` objective minimizes the expected loss:

$$\mathbb{E}_{x_0, t, \epsilon, w} \left[\left\| \epsilon_{\theta}(x_t | c, w, \mathcal{D}^T) - (\epsilon + (w - 1) \cdot \Delta(x_t, c, \mathcal{D}^T)) \right\|^2 \right]. \quad (18)$$

Assuming that $\epsilon_{\theta}(x_t | c, w)$ is linear in w , we can write the model as:

$$\epsilon_{\theta}(x_t | c, w, \mathcal{D}^T) = A + B \cdot (w - 1). \quad (19)$$

Since the training loss is a squared error between two linear functions of w , minimizing this loss for all values of w is equivalent to matching the corresponding coefficients of both functions. That is, to minimize the loss over the full support of w , the model must satisfy:

$$A = \epsilon, \quad B = \Delta(x_t, c, \mathcal{D}^T). \quad (20)$$

Since $\epsilon_{\theta}(x_t | c, \mathcal{D}^T) \approx \epsilon_{\theta}(x_t | c, w = 1, \mathcal{D}^T) \approx \epsilon$, this gives the optimal solution:

$$\epsilon_{\theta}(x_t | c, w, \mathcal{D}^T) = \epsilon + (w - 1) \cdot (\epsilon_{\theta}(x_t | c, \mathcal{D}^T) - \epsilon_{\theta_0}(x_t)), \quad (21)$$

which matches the DoG direction used at test time. Therefore, `DogFit` learns to internalize the DoG guidance signal during training, removing the need for external guidance at sampling. ■

Proposition 2. `DogFit` implicitly augments MG’s training process with a classifier-based domain alignment term:

$$\epsilon'_{\text{DogFit}} = \epsilon'_{\text{MG}} - \sigma(w - 1) \cdot \nabla_{x_t} \log p_{\theta}(\mathcal{D}^T | x_t). \quad (22)$$

This enables `DogFit` to retain MG’s class-conditional guidance while avoiding out-of-distribution generation by pulling samples toward the core of the target domain manifold.

Proof sketch. The target noise in MG, when applied in the task of fine-tuning, can be rewritten as:

$$\epsilon'_{\text{MG}} = \epsilon + (w - 1) \cdot \text{sg}(\epsilon_{\theta}(x_t | c, \mathcal{D}^T) - \epsilon_{\theta}(x_t | \mathcal{D}^T)). \quad (23)$$

Then, by subtracting the target noise values of MG and `DogFit`, we have:

$$\epsilon'_{\text{DogFit}} - \epsilon'_{\text{MG}} = (w - 1) \cdot \text{sg}(\epsilon_{\theta}(x_t | \mathcal{D}^T) - \epsilon_{\theta_0}(x_t)). \quad (24)$$

According to Equations 12 and 13, Equation 24 can be rewritten as:

$$= -\sigma(w - 1) \cdot \text{sg}(\nabla_{x_t} \log p_{\theta}(x_t | \mathcal{D}^T) - \nabla_{x_t} \log p_{\theta}(x_t)) \quad (25)$$

By Bayes’ rule, we have:

$$\frac{p(x_t | \mathcal{D}^T)}{p(x_t)} \propto p(\mathcal{D}^T | x_t), \quad (26)$$

which is equivalent to:

$$\nabla_{x_t} \log p(\mathcal{D}^T | x_t) = \nabla_{x_t} \log p_t(x_t | \mathcal{D}^T) - \nabla_{x_t} \log p_t(x_t). \quad (27)$$

Thus, given that MG uses $\epsilon_{\theta}(x_t | \mathcal{D}^T)$ as an approximation to $-\sigma_t \nabla_{x_t} \log p(x_t | \mathcal{D}^T)$, we can express `DogFit` as applying MG, but with a correction term that pushes towards a target domain classifier’s gradient direction. ■

Additional Experiments

FID Sensitivity to w without Controllability

We further examine the sensitivity of our method to w in the absence of controllability. We train a specific model for each w and compare the FID trends of `DogFit` and DoG across varying values (Fig. 10). While both methods achieve optimal FID in a similar range, `DogFit` exhibits a sharper degradation for larger w , suggesting higher sensitivity to strong guidance values. We hypothesize that this is due to training-time overexposure to extreme guidance, which can lead the model to learn from unnatural signals that do not follow the real target distribution, thereby reducing generation quality. This motivates our choice of sampling w from an exponentially decaying distribution, ensuring the model is only sparsely exposed to high guidance values during training.

Controllable Guidance Analysis on Cars

Fig. 8 provides an extended version of the controllable guidance analysis for the Stanford-Cars dataset. This complements the main findings and illustrates the same trends on a new domain.

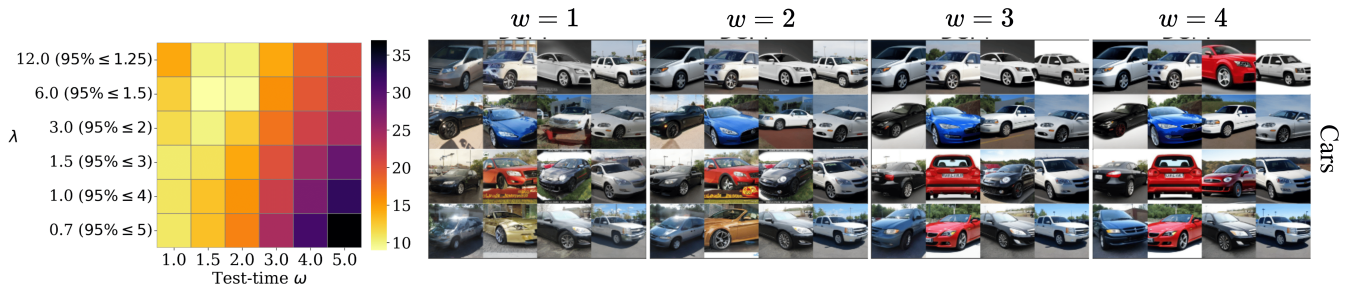


Figure 8: Effect of controllable guidance at test time for the Stanford-Cars domain. (Left) FID heatmaps showing the behaviour of FID given different test-time w s with different training-time λ s. (Right) Corresponding generated samples for fixed $\lambda = 3$ (i.e., 95% of sampled w values lie between 1 and 2), across varying test-time w .

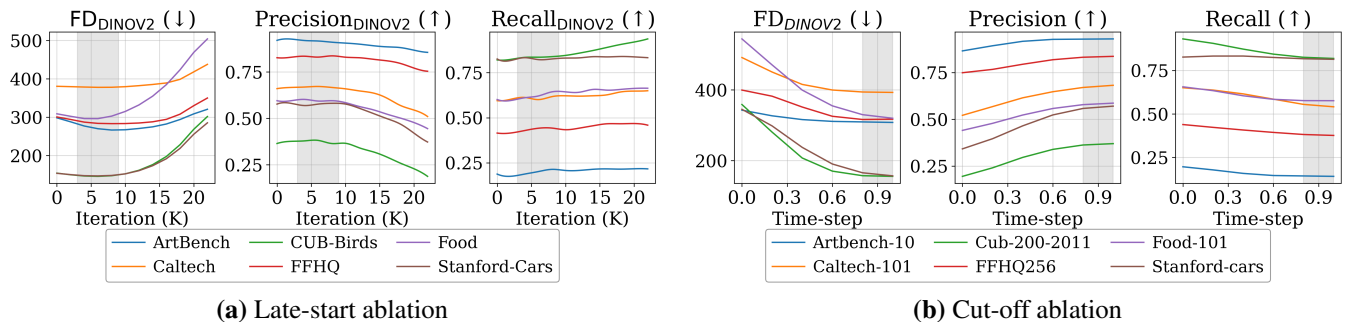


Figure 9: Ablation study on guidance schedules in `DogFit`. (a) Varying the late-start threshold τ_s to control when guidance begins. (b) Varying the cut-off threshold τ_c to restrict guidance to later denoising steps. Performed using FD_{DINOv2} on `DiT-XL/2`.

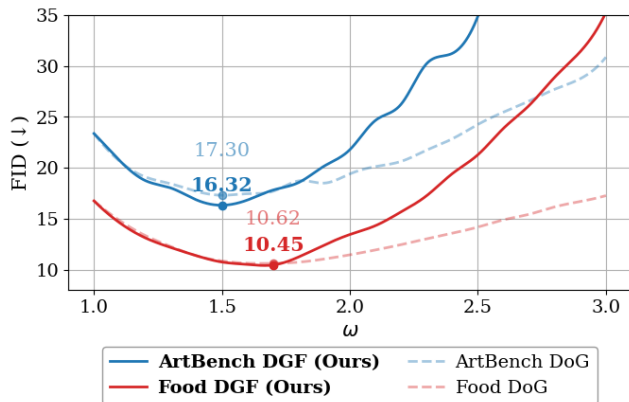


Figure 10: Comparing `DogFit` (without guidance control) and `DoG` in sensitivity of FID to w .

Guidance Scheduling on FD_{DINOv2}

We observe that delaying guidance using the late-start strategy improves both FD_{DINOv2} and precision, consistent with our FID-based findings. This supports the idea that postponing guidance allows for stronger and more accurate directional signals once the model has sufficiently stabilized (Fig. 9a). However, unlike FID, applying the cut-off strategy—where guidance is limited to later denois-

ing steps—shows little to no improvement in FD_{DINOv2} across most domains (Fig. 9 (b)). We believe this is due to a fundamental difference in what the two metrics capture: FID benefits from preserving the global structure inherited from the source model, which is often formed early in the denoising process. In contrast, FD_{DINOv2} focuses more on semantic alignment with the target domain, which may require guidance to be present throughout the generation, not just in the later steps. This distinction further highlights the importance of using multiple metrics when evaluating generative models.

Qualitative Comparison on `SiT-XL/2`

Fig. 11 provides a qualitative comparison on the `SiT-XL/2` backbone. `DogFit` generates sharp, domain-relevant details on par with `DoG`, while avoiding out-of-distribution behavior occasionally seen with `CFG` and `MG` (e.g., distorted faces and birds).

Precision and Recall Analysis

Tab.4 presents a comparison of Precision and Recall (Kynkäänniemi et al. 2019) between `DogFit` and the baselines on the `DiT-XL/2` backbone. Precision reflects the fidelity or quality of generated samples, while Recall measures sample diversity. As expected, all guidance methods consistently improve Precision compared to finetuning while reducing Recall, aligning with the general behavior of

Table 4: Precision and Recall results on DiT/XL-2 backbone using Inception and DINOv2 metrics.

Metric	Method	Unlabelled	Labelled					
		FFHQ	ArtBench	Caltech	CUB-Birds	Food	Stanford-Cars	Avg.
Precision (Inception)	Fine-tuning	0.70	0.67	0.60	0.58	0.79	0.51	0.63
	+ CFG (Ho and Salimans 2022)	-	0.68	0.76	0.72	0.82	0.63	0.72
	+ DoG (Zhong et al. 2025)	0.83	0.77	0.81	<u>0.82</u>	0.88	<u>0.77</u>	0.81
	MG (Tang et al. 2025)	-	0.68	0.76	0.71	0.81	0.62	0.72
	DogFit	<u>0.81</u>	<u>0.76</u>	<u>0.75</u>	<u>0.82</u>	<u>0.87</u>	<u>0.74</u>	<u>0.79</u>
	DogFit + Control	0.83	<u>0.76</u>	<u>0.78</u>	0.83	<u>0.87</u>	0.80	0.81
Precision (DINOv2)	Fine-tuning	0.74	0.84	0.48	0.16	0.41	0.30	0.44
	+ CFG (Ho and Salimans 2022)	-	0.83	<u>0.67</u>	0.30	0.48	0.47	0.52
	+ DoG (Zhong et al. 2025)	0.82	<u>0.91</u>	0.73	0.39	0.59	0.61	0.65
	MG (Tang et al. 2025)	-	0.84	0.63	0.28	0.51	0.44	0.54
	DogFit	<u>0.83</u>	0.92	<u>0.67</u>	<u>0.38</u>	<u>0.58</u>	0.58	<u>0.62</u>
	DogFit + Control	0.86	0.90	<u>0.67</u>	<u>0.38</u>	<u>0.58</u>	<u>0.59</u>	<u>0.62</u>
Recall (Inception)	Fine-tuning	0.67	0.57	0.75	0.81	0.52	<u>0.58</u>	0.65
	+ CFG (Ho and Salimans 2022)	-	<u>0.56</u>	0.66	<u>0.76</u>	<u>0.53</u>	0.59	0.62
	+ DoG (Zhong et al. 2025)	0.61	0.50	0.65	0.68	0.48	0.52	0.57
	MG (Tang et al. 2025)	-	<u>0.56</u>	0.67	0.75	0.55	0.59	<u>0.624</u>
	DogFit	<u>0.63</u>	0.51	<u>0.70</u>	0.68	0.50	0.55	0.59
	DogFit + Control	0.57	0.51	0.68	0.67	0.50	0.48	0.57
Recall (DINOv2)	Fine-tuning	0.46	0.21	0.66	0.95	0.67	0.82	0.66
	+ CFG (Ho and Salimans 2022)	-	0.22	0.59	0.87	0.61	0.84	<u>0.63</u>
	+ DoG (Zhong et al. 2025)	<u>0.44</u>	0.21	0.57	0.83	<u>0.64</u>	0.83	0.62
	MG (Tang et al. 2025)	-	0.22	0.60	0.89	0.60	0.84	<u>0.63</u>
	DogFit	0.43	0.21	0.60	0.83	<u>0.64</u>	0.83	0.62
	DogFit + Control	0.43	0.21	<u>0.61</u>	0.85	<u>0.64</u>	0.83	<u>0.63</u>

guided diffusion models. This effect arises because guidance steers sampling toward high-likelihood regions of the conditional distribution, which inherently narrows the output distribution and suppresses diversity. Our method, both with and without guidance control, matches the performance of DoG in terms of both Precision and Recall in most settings. Notably, DogFit achieves the highest or second-highest Precision in both Inception and DINOv2 metrics across all datasets). In terms of Recall, DogFit and DoG slightly underperform CFG and MG, which we believe is due to the additional domain alignment term further reducing the diversity to prevent out-of-domain target generations (Equation 22). While recent works explore diversity-preserving techniques and scheduling mechanisms for guidance during sampling (Kynkäänniemi et al. 2024; Sadat et al. 2023), analogous techniques for training-time guidance have yet to be developed. We leave the exploration of such methods for training-guided models like DogFit as an exciting direction for future work.

Scaling to Large Resolutions

Tab.6 provides a comparison between DogFit and CFG when fine-tuning DiT-XL/2 pretrained at 512×512 on Food101 (Bossard, Guillaumin, and Van Gool 2014) at 512×512 . Results indicate that DogFit is fully scalable to

larger resolutions, broadening its applicability and demonstrating invariance to image scale. For this experiment, we use a batch size of 12 and use the same hyperparameters as in our main experiments.

Robustness to Stronger Domain Shifts

While our target datasets span a range of distribution gaps, we additionally evaluate transfer on the EuroSat dataset (Helber et al. 2019), consisting of 27,000 satellite images with 10 classes, which shares very few features with the source domain. This setting probes whether DogFit’s source prior still provides a better signal than that of the fine-tuned target under extreme shift. We note that as the target domain diverges substantially from the source, the advantages of transfer learning from the source generally diminishes relative to training on the target data from scratch. Nevertheless, our results in Tab.7 show that DogFit still outperforms Fine-tuning and CFG in this case, indicating that leveraging the source prior can still improve generation quality even when transfer benefits are attenuated.

Exponential vs. Uniform Scheduling

Tab.7 shows that sampling the guidance weight ω from a SEDD (Fig. 7) consistently outperforms uniform schedules across all test-time values of ω . In particular, SEDD yields

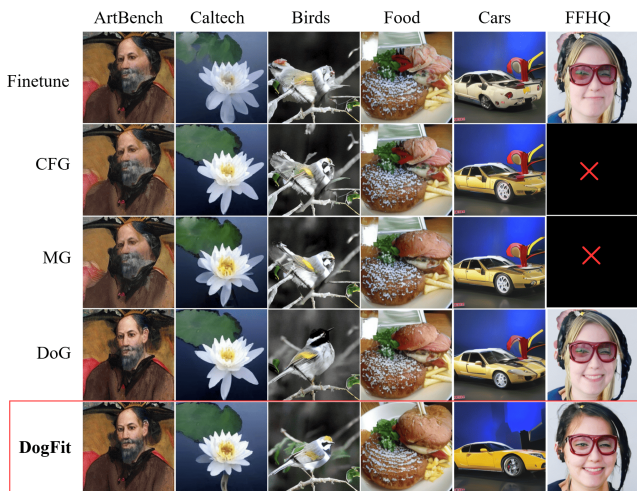


Figure 11: Qualitative comparison of guidance mechanisms on SiT-XL/2 (guidance scale 1.5). \times : not applicable.

Test-time ω	Uniform				SEDD ($\lambda = 2$)
	$\mathcal{U}[1, 1.1]$	$\mathcal{U}[1, 1.25]$	$\mathcal{U}[1, 1.5]$	$\mathcal{U}[1, 2]$	
1	19.02	16.68	20.08	22.08	12.98
1.5	19.62	13.84	18.27	18.05	10.94
2	29.65	15.97	26.29	24.23	13.05
3	61.56	28.28	53.28	48.00	19.81
4	85.62	53.24	70.60	65.12	24.84
5	114.97	98.75	88.39	77.53	27.95

Table 5: Ablating training-time guidance sampling methods, by comparing SEDD and uniform sampling. Results indicate FID \downarrow across a wide range of test-time ω values.

lower FID while uniform sampling over broader ranges destabilizes learning and collapses diversity, with FID inflating as ω increases. This empirical trend aligns with our linearity assumption in **Proposition 1** which leads to the equivalence of DogFit and DoG (Zhong et al. 2025) under small ω values (Zheng and Lan 2023). By concentrating the probability mass near $\omega \approx 1$, SEDD keeps optimization within the proposition’s validity region, preserving the expected guidance behavior and allowing the use of larger test-time guidance values during generation.

DogFit in Text-to-Image Transfer Learning

To further show the broad applicability of our method, we show the efficacy of DogFit in two different text-to-image experiments, Dreambooth subject driven transfer (Ruiz et al. 2023), and LoRA style transfer (Hu et al. 2022) to Pokémon. Note that these settings typically require large guidance values of up to 7.5 for the model to produce visually pleasing images. However, DogFit is more theoretically grounded when exposed to small-guidance values during training, where it locally matches DoG (Zhong et al. 2025) (see Proposition 1). While controllable guidance (conditioning on w) is a natural extension allowing for large test-time ω values, we focus here on fixed guidance during training due to limited time and leave that extension for fu-

Method	FID \downarrow	KID $\downarrow (\times 10^{-4})$	FD _{DINOv2} \downarrow	#Pass
Fine-tuning	15.73	90.41	510.60	x1
+ CFG	11.93 (+24.16%)	57.69 (+36.19%)	366.00 (+28.32%)	x2
DogFit	11.06 (+29.69%)	43.15 (+52.27%)	380.44 (+25.49%)	x1

Table 6: Adapting DiT-XL/2 to Food101 at 512 \times 512 resolution. Percent improvements relative to Fine-tuning are in parentheses.

Method	FID \downarrow	KID $\downarrow (\times 10^{-4})$	FD _{DINOv2} \downarrow	#Pass
Fine-tuning	36.08	24.23	258.62	x1
+ CFG	33.38 (+7.48%)	21.25 (+12.30%)	257.73 (+0.34%)	x2
DogFit	29.30 (+18.79%)	16.51 (+31.86%)	221.03 (+14.53%)	x1

Table 7: Adapting DiT-XL/2 to the distant EuroSat domain at 256 \times 256.

ture work. Despite this conservative setting, DogFit significantly improves unguided fine-tuning with small guidance values ($\omega = [1.65, 1.75]$) and approaches the performance of CFG with high guidance value ($\omega = 7.5$).

DreamBooth (subject-driven transfer). We apply Dreambooth fine-tuning on Stable Diffusion v1.5 (Rombach et al. 2022; Podell et al. 2023) to new subjects using a handful of instance images with DogFit. In this regime, the fine-tuning prompts are typically limited to templates such as “a [v] photo of {subject}”, while at inference we expect the model to respond to diverse prompts from the source domain. This mismatch makes faithful distillation of text-conditioning challenging. Nevertheless, Fig. 12 and Tab. 8 show that DogFit learns controllable alignment with the prompt and significantly outperforms unguided fine-tuning while approaching CFG on DINO, CLIP-I, and CLIP-T, the standard metrics for subject-driven generation (Ruiz et al. 2023).

LoRA fine-tuning on Pokémon (style transfer). We adapt Stable Diffusion v1.5 to the Pokémon style dataset¹ with 833 image–caption pairs. We train a LoRA adapter (rank 4) for 2,000 iterations at a learning rate of 10^{-4} . We evaluate with CLIP-T over the first 100 prompts (one image per prompt). As summarized in Tab.9, DogFit significantly improves prompt alignment over unguided fine-tuning while using a small guidance value ($\omega=1.75$) and a single sampling pass, and it closely approaches CFG which requires two passes and a large guidance value ($\omega=7.5$).

¹<https://huggingface.co/datasets/diffusers/pokemon-gpt4-captions>

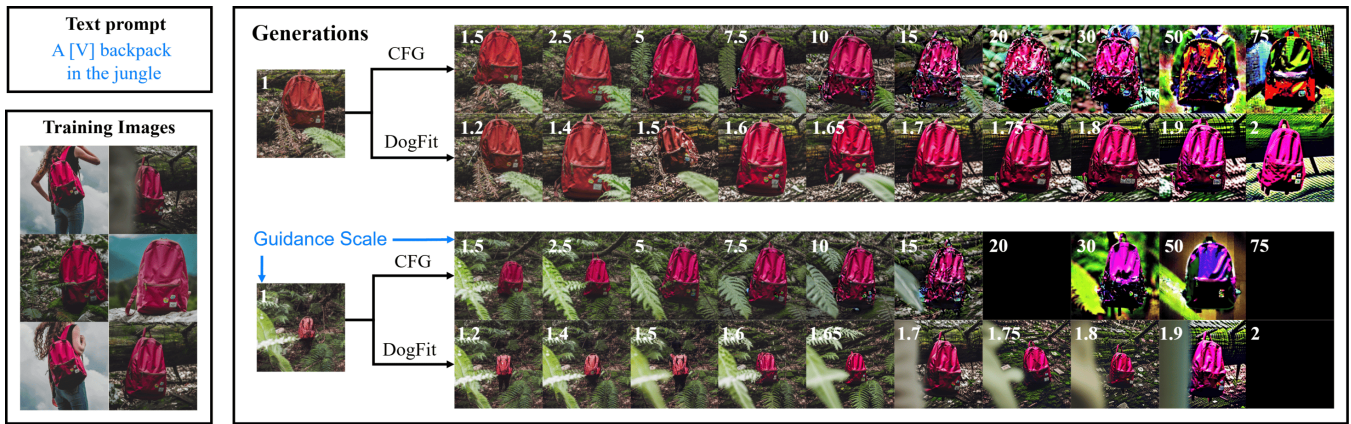


Figure 12: Qualitative DreamBooth text-to-image generations (SD v1.5) comparing CFG and DogFit. Black images correspond to Not-Safe-For-Work (NSFW) content detection using hugging face generators.

Method	DINO \uparrow	CLIP-I \uparrow	CLIP-T \uparrow	#Pass
Fine-tuning	0.383	0.697	0.275	x1
+ CFG	0.529 (+38.1%)	0.799 (+14.6%)	0.304 (+10.5%)	x2
DogFit	0.516 (+34.7%)	0.758 (+8.8%)	0.269 (-2.2%)	x1

Table 8: Comparison on the text-to-image DreamBooth benchmark for fine-tuning Stable Diffusion V1.5. Results are based on the best guidance strength per method ($\omega_{\text{CFG}} = 7.5$, $\omega_{\text{DogFit}} = 1.65$).

Guidance	CLIP-T \uparrow	#Pass
Real data	0.347	-
Fine-tuning	0.276	x1
+ CFG	0.343 (+24.3%)	x2
DogFit	0.319 (+15.6%)	x1

Table 9: Comparison on text-to-image LoRA fine-tuning of Stable Diffusion v1.5 to the Pokémon image-caption dataset. Results are based on the best guidance strength per method ($\omega_{\text{CFG}} = 7.5$, $\omega_{\text{DogFit}} = 1.75$).